Homaeigohar, S.S.; Elbahri, M.:

Novel compaction resistant and ductile nanocomposite nanofibrous microfiltration membranes

In: Journal of Colloid and Interface Science (2011) Elsevier

DOI: 10.1016/j.jcis.2012.01.012

Novel Compaction Resistant and Ductile Nanocomposite Nanofibrous Microfiltration Membranes

Seyed Shahin Homaeigohar [a] and Mady Elbahri[*a,b]

a: Helmholtz-Zentrum Geesthacht (HZG), Institute of Polymer Research, Nanochemistry and Nanoengineering group, Max-Planck-Str. 1, 21502 Geesthacht, Germany

b: Nanochemistry and Nanoengineering group, Institute for Materials Science, Faculty of Engineering, University of Kiel, Kaiserstrasse 2,24143 Kiel, Germany

* To whom correspondence should be addressed:

E-mail: mady.elbahri@hzg.de

Tel: +494152872802

Fax: +494152872499

Abstract

Despite promising filtration abilities, low mechanical properties of extraordinary porous electrospun nanofibrous membranes could be a major challenge in their industrial development. In addition, such kind of membranes are usually hydrophobic and non-wettable. To reinforce an electrospun nanofibrous membrane made of polyethersulfone (PES) mechanically and chemically (to improve wettability), zirconia nanoparticles as a novel nanofiller in membrane technology were added to the nanofibers.

The compressive and tensile results obtained through nanoindentation and tensile tests, respectively, implied an optimum mechanical properties after incorporation of zirconia nanoparticles. Especially compaction resistance of the electrospun nanofibrous membranes improved significantly as long as no agglomeration of the nanoparticles occurred and the electrospun nanocomposite membranes showed a higher tensile properties without any brittleness i.e. a high ductility. Noteworthy, for the first time the compaction level was quantified through a nanoindentation test. In addition to obtaining a desired mechanical performance, the hydrophobicity declined. Combination of promising properties of optimum mechanical and surface chemical properties led to a considerably high water permeability also retention efficiency of the nanocomposite PES nanofibrous membranes. Such finding implies a longer life span and lower energy consumption for a water filtration process.

Keywords: electrospinning; membrane; nanocomposite nanofiber; mechanical properties; transport properties

1. Introduction

Electrospinning is undoubtedly an efficient processing method to manufacture nanofibrous structures useful for a number of applications such as filtration [1]. Electrospun nanofibrous mats are highly porous with interconnected pores in the size range of only a few times to a few ten times the fiber diameter. The promising structural features make them strong candidates for filtration applications. The high porosity implies a higher permeability and the interconnected pores can withstand fouling better. Furthermore, the small pore size of the nanofibrous membranes could be beneficial in term of a high retention [2]. Despite promising filtration features, an electrospun membrane which is exposed to various stresses applied by fluid flow should also possess sufficient mechanical strength [3]. Without mechanical stability, the membrane undergoes mechanical failures such as compaction which affects the filtration efficiency. Hence, mechanical strengthening of the electrospun nanofibrous membranes could be a very critical objective to broaden the range of their applications.

In our previous study on a polyethersulfone (PES) electrospun nanofibrous membrane, water flux measurements indicated that when pressure difference over the membrane increases e.g. in a multi layer filtration system, compaction of the electrospun nanofibrous layer during filtration decreases the permeability [4]. The occurrence of such mechanical failure necessitates enhancement of the mechanical properties of the PES electrospun nanofibrous membrane.

In order to meet the requirement mentioned above, several approaches such as heat treatment [4-6] and solvent induced interfiber bonding [3] have been taken by the researchers to reinforce electrospun nanofibrous mats.

Another approach could be the nanocomposite strategy. As we know, incorporation of nanoparticles into polymeric materials can improve the mechanical properties of the composites. As an example, in the rubber industry the mechanical strength of rubber composites has been optimized using nanoparticular fillers (e.g. carbon black) for nearly a century [7]. This idea can also be applicable for electrospun nanofibers used as filtration membranes to lower their compaction. In our previous research [8], we could demonstrate that addition of sol-gel formed TiO_2 nanoparticles to an electrospun nanofibrous membrane could be beneficial in terms of tensile mechanical properties as well as hydrophilicity. However, the performance of the membrane under compressive stresses, i.e. the compaction resistance, during a pressure-driven liquid filtration process, such as microfiltration, was still unknown. In our new forthcoming study, for the first time the compaction resistance of an electrospun membrane which is especially of a significant importance during a dead-end filtration mode will be studied i.e. quantified and improved through addition of zirconia nanoparticles as a novel nanofiller in membrane technology [9, 10].

Zirconia is a known inorganic material that through a phase transformation toughening mechanism exhibits the most optimum mechanical properties of oxide ceramics. The mechanical stresses induce a phase transformation from metastable tetragonal grains to the monoclinic phase at the crack tip. This transformation is accompanied by volume expansion inducing compressive stresses and suppressing crack propagation [11]. Despite the promising mechanical properties, zirconia has been used only for a few applications in the membrane industry e.g. as a bulk material in organo-mineral (polysulfone and polyvinylidene fluoride) ultrafiltration membranes. In such

applications, zirconia has been utilized with grain sizes in the micrometer range and the properties and effects have never been examined at the nanoscale [9, 10].

Here we show for the first time that PES electrospun nanofibrous membranes reinforced with zirconia nanoparticles below a certain amount can resist against mechanical stresses and compaction without any brittleness. By such a way, the membranes' porous structure will be preserved. High volume porosity along with improved wettability due to the presence of these ceramic nanoparticles lead to a significantly improved performance in water filtration.

In the current study, PES was selected as the membrane material due to its high thermal and chemical resistance as well as its appropriate mechanical properties. Also, PES can be considered as a model membrane material as it is widely used for commercial microfiltration and ultrafiltration membranes.

In the forthcoming research, the effect of addition of zirconia nanoparticles on morphological properties including fibers' diameter and surface roughness, and distribution mode of the nanoparticles inside the nanofibers will be investigated by SEM and TEM, respectively. Any change in porosity and pore size of the nanofibrous membranes will be quantified. More importantly, mechanical performance of the nanocomposite PES nanofibrous membranes is characterized under compressive and tensile forces by nanoindentation, tensile test and dynamic mechanical analysis (DMA). Moreover, water contact angle measurements can show any alteration in hydrophobicity of the membranes by addition of zirconia nanoparticles. Finally, water flux measurements and retention tests based on filtration of a colloidal nanosuspension can prove the

probable improvement of filtration efficiency of the reinforced PES nanofibrous membranes.

2. Materials and methods

2.1. Materials

Polyethersulfone Ultrason E6020P (M_w= 58,000 and density of 1.37 g/cm^3) was purchased from BASF (Germany). The solvent *N*,*N*-dimethylformamide (DMF) was obtained from Merck (Germany). Zirconium oxide (zirconia) powder with average particle size of 29–68 nm was supplied from Nanoamor Co.(USA). To investigate the retention ability of the membranes, as the suspended solids in water to be filtered out, Titania nanoparticles were also purchased from Degussa (Japan). All materials were used as received.

2.2. Preparation of ZrO_2/PES electrospun nanofibrous mats

For preparation of the PES solution containing zirconia nanoparticles, a two-step method was used. Initially the nano-zirconia (1.0, 5.0, 7.0 wt.%) was dispersed in DMF by magnetic stirring and ultrasonicated at room temperature for 105 min to disrupt possible agglomerates. The average particle size of zirconia particles dispersed in DMF was determined by a particle size analyzer (Delsa C™ Nano particle size analyzer, Beckman Coulter, USA) based on a photon correlation spectroscopy (PCS) method.

In the second step, the appropriate weight of PES flakes was added to the ZrO_2/DMF dispersion. This was followed by magnetic stirring until the polymer dissolved completely.

The ZrO_2/PES nanofibrous mats were produced by an electrospinning method of the prepared solution. Briefly, the solution (20 wt%) was fed with a constant rate of 0.5 mL/h into a needle by using a syringe pump (Harvard Apparatus, USA). By applying a voltage of 20-25 kV (Heinzinger Electronic GmbH, Germany) electrospinning was done on an Aluminum (Al) foil located 25 cm above the needle tip for 8 hours. In contrary to the solutions containing no and lower filler amount i.e. 1wt%, those with the higher contents needed a larger voltage in the mentioned range.

To facilitate the next discussions, the nanocomposite fibrous membranes will be abbreviated as NFM1, NFM5 and NFM7 in which the value mentioned at the end represents the theoretical amount of the nanofiller added.

2.3. Morphological characterization

The morphology of the neat PES electrospun nanofibers and those doped with zirconia nanoparticles was observed by scanning electron microscope (SEM) (LEO 1550VP Gemini from Carl ZEISS) after a gold coating and at an acceleration voltage of 3 kV. Additionally, the distribution mode of the nanoparticles incorporated into the nanofibers was investigated through transmission electron microscopy (TEM) (Tecnai G2 F20 field emission at an acceleration voltage of 200kV).

The thickness of the nanofibrous mats for all the mechanical tests was measured using a digital micrometer (Deltascope® MP2C from Fischer). The diameter of the electrospun nanofibers was determined from the SEM images using the Adobe Acrobat v.07 software.

2.4. Mechanical characterization (Nanoindentation)

To investigate the compressive mechanical performance of the ZrO_2/PES electrospun nanofibrous mats, nanoindentation testing was performed. Indentation tests were conducted using a Nanoindenter XP (MTS system Co., MN, USA) utilizing a conical diamond flat punch indenter (diameter of 50 μm and angle of 60°) with a continuous stiffness measurement (CSM) technique. The nanoindentation tests were carried out as follows: a displacement rate of 100 nm/s was maintained constant during the increment of load until the indenter reached 10,000 nm deep into the surface. The load was then held at maximum value for 10 s in order to avoid creep significantly affecting the unloading behavior. The indenter was then withdrawn from the surface at the unloading rate of 0.1 mN/s. At least 20 indents were performed on each sample and the distance between the indentations was 200 μm to avoid interaction.

2.5. Mechanical characterization (tensile test)

The ZrO_2/PES nanofibrous mats were carefully cut into rectangular strips with dimensions of 10 mm x 80 mm and thickness of 120-140μm. The tensile properties were characterized by a tensile machine (Zwick/Roell Z020-20KN, Germany) equipped with a 20-N load-cell at ambient temperature. The cross-head speed was 2 mm/min and the gauge length was 20 mm. The reported tensile moduli, tensile strengths and elongations represented average results of ten tests.

2.6. Mechanical characterization (DMA)

The frequency-dependant elastic moduli of the ZrO_2/PES electrospun nanofibrous mats was measured using a dynamic mechanical analyzer (RSA II, Rheometrics Co.) equipped with a tensile fixture.

The electrospun nanofibrous samples were cut as 23 mm x 3.9 mm with a thickness of 130 μm.

Briefly, the frequency-dependent mechanical properties were investigated at ambient temperature, with a frequency sweep from 0.005 to 100 rad/s using a deformation amplitude of 0.5%.

2.7. Water contact angle measurement

The static water contact angle of the ZrO_2/PES nanofibrous membranes was measured using a contact angle analysis system (Kruess DSA 100, Germany). A 5 μl droplet was dispensed on the membrane and the resultant angle was measured.

2.8. Porosity and pore size measurement

For the porosity measurement, circular- shape pieces of the electrospun mats with known area were stamped out and their thickness and mass were accurately measured using a digital micrometer and an electronic balance (a resolution of 0.1 mg), respectively. The apparent density (ρ) of the electrospun mats was calculated from the obtained mass and the volume (in a compacted form owing to the pressure of the micrometer tip measuring the thickness of the mat). Then the porosity of the electrospun membranes was determined according to the equation (1)[12]:

$$\varepsilon = \frac{(\rho_0 - \rho)}{\rho_0} \times 100\% \quad (1)$$

Where ε is porosity, ρ_0 and ρ are the average density of the materials used in electrospinning and apparent density of the electrospun mats, respectively. ρ_0 can be calculated according to the equation (2):

$$\frac{1}{\rho_0} = \frac{\phi_{PES}}{\rho_{PES}} + \frac{\phi_{ZrO_2}}{\rho_{ZrO_2}} \quad (2)$$

Where ρ_{PES} and ρ_{ZrO_2} are 1.37 and 5.68 g/cm^3 , respectively. ϕ_{PES} and ϕ_{ZrO_2} are mass fractions of the components.

Subsequently, based on the measured nanofiber diameters (d)(nm) and porosities (ε)(-), the mean pore radius ($\bar{r}$) of the electrospun nanofibrous membranes was calculated according to the equation (3)[13, 14]:

$$\bar{r} = \frac{\sqrt{\pi}}{4}\left(\frac{\pi}{2\log(\frac{1}{\varepsilon})} - 1\right)d \quad (3)$$

2.9. Water flux measurement

Membrane permeability was characterized through a pure water dead-end filtration (the set-up already shown in [8]). The dried membrane (2 cm^2) was placed in the membrane module and the water in the reservoir (300 ml) was passed through by applying a feed pressure of 0.5 bar. The time required for permeation of the water through the membranes was recorded and the flux according to Eq. (4) was calculated :

$$J = \frac{Q}{A.\Delta t} \quad (4)$$

where J is the permeation flux (L/m^2.h), Q is the permeated volume (L) of water, A is the effective area of the membranes (m^2), and Δt is the sampling time (h). The flux measurement tests were repeated three times.

2.10 Retention test using an inorganic nanosuspeniosn

The retention capability of the electrospun fibrous membranes for colloidal particles was determined using TiO_2 aqueous nanosuspensions.

The dried membranes were placed in the membrane module of the custom-built set-up used previously for water flux measurement. The reservoir of the set-up was filled with a TiO_2 heterodisperse suspension (0.06 g/L) to be passed through the membranes by applying a feed pressure of 0.5 bar. The retention ability was probed by the eventual presence and size of the remaining nanoparticles in the permeate suspension. The average particle size of the TiO_2 nanoparticles present in the feed and permeates (50 mL) was determined by using a particle size analyzer (Delsa C ™ Nano particle size analyzer, Beckman Coulter, USA). Moreover, to calculate the permeate flux according to the equation (4), the permeation time was also recorded.

3. Results and discussion

3.1. Morphological Properties

As the presence of zirconia nanoparticles might affect the morphological properties (for example by bead formation) of the electrospun nanofibers, Scanning

electron micrographs (SEM) were taken of the PES electrospun nanofibers with and without zirconia particles (Fig. 1 A-D).

According to the SEM images, the nanoparticles were not visible on the surface of the nanofibers implying their encapsulation inside the nanofibers. Furthermore, no bead formation was observed for the nanocomposite fibers of all compositions compared to the neat ones.

While addition of the inorganic filler increases the viscosity and viscoelastic force, it hampers the surface tension of the PES solution to be electrospun. Consequently, formation of structural irregularities such as beads and surface roughness decreases and the fiber diameter distribution becomes more uniform [15]. However, higher viscoelastic force leads to a higher resistance toward electrostatic force stretching the jet. As seen in Fig. 1E, at the higher nanofiller concentrations this effect magnifies the fiber diameter [2, 16]. Owing to a higher nanofiller content, the highest viscoelastic force is seen at 7 wt% zirconia which inhibits a continuous jet formation. Hence, to continue electrospinning a higher voltage is needed which subsequently leads to the nanofibers, which are thinner, and possess rougher and more porous surface in comparison to the former composition i.e. 5 wt% electrospun at a lower voltage (Fig. 2 B Vs. 2A) [17].

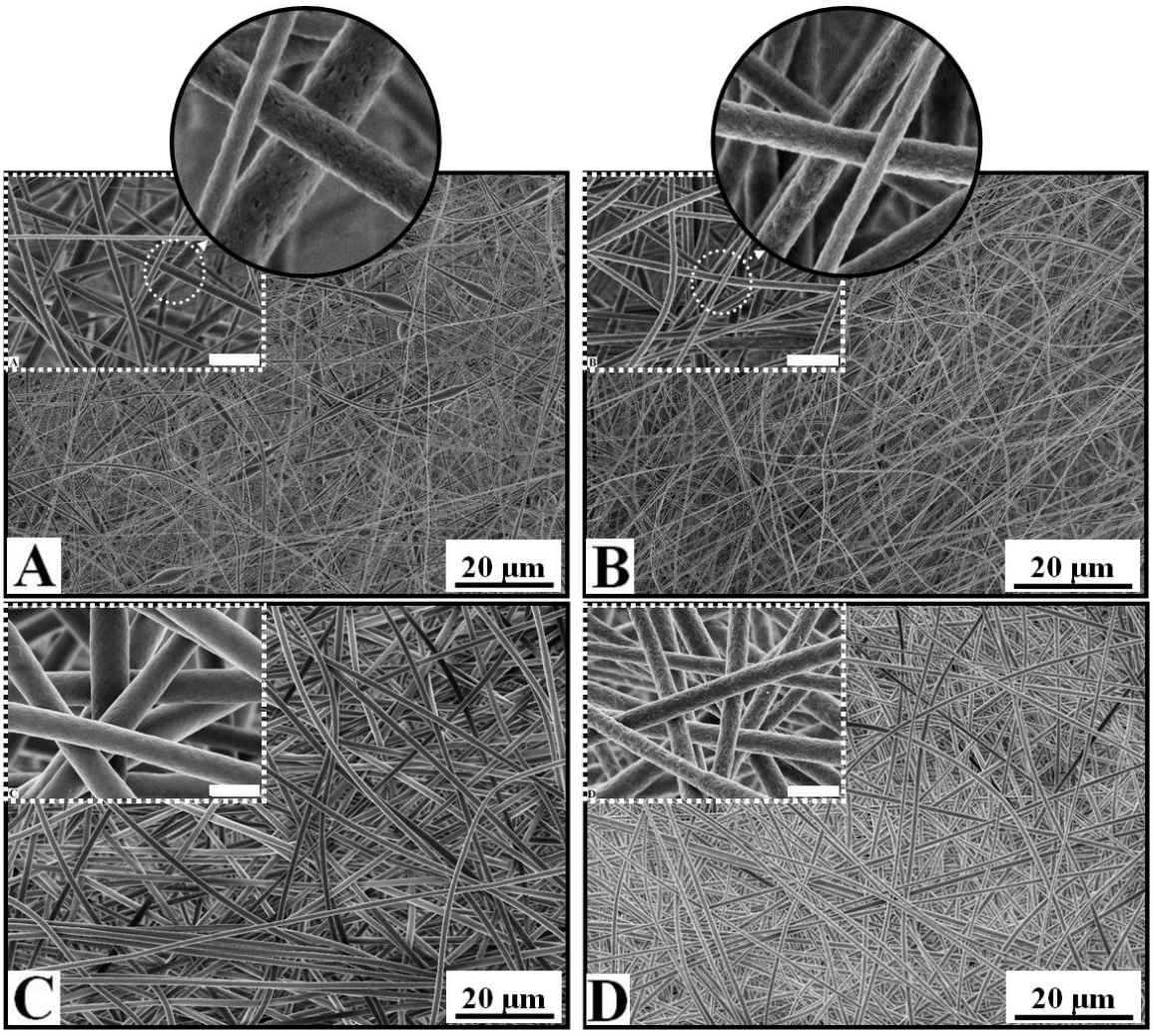

Fig. 1

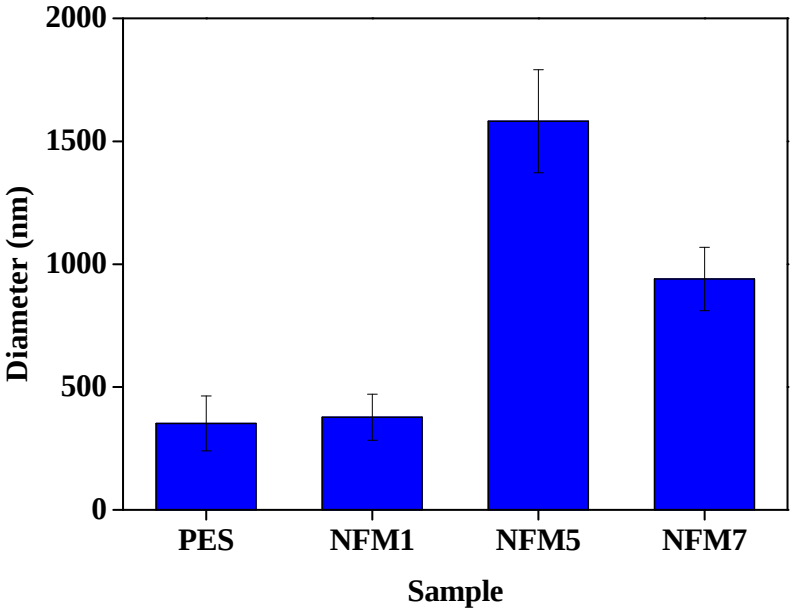

(E)

Fig. 1

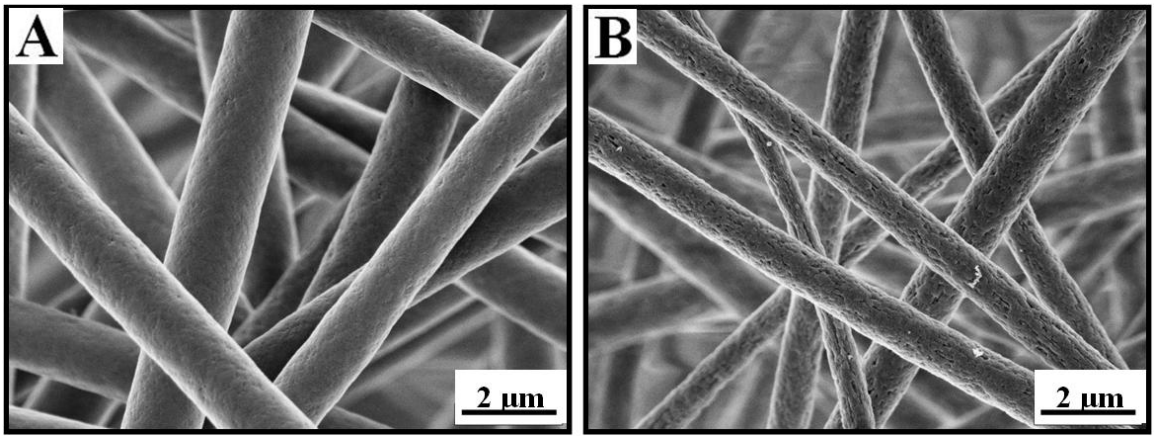

Fig. 2

In term of particle size distribution, as shown in Fig. 3A, agglomeration of the primary zirconia nanoparticles present in the solution to be electrospun despite ultrasonication and stirring is inevitable. The average particle size for 1, 5 and 7 wt% zirconia is 130, 420 and 260 nm, respectively. Other than 1 wt% zirconia, the two other

concentrations show a broad distribution mode (polydispersity indices (PIs) for 1, 5 and 7 wt% zirconia are 0.08, 0.16 and 0.25, respectively). However, surprisingly, unlike the particle size analysis results implying agglomeration, the TEM observations confirmed the presence of zirconia nanoparticles embedded into the nanofibers approximately with their original size of ~ 29–68 nm i.e. negligible agglomeration (Figs. 3B&C). During electrospinning, the viscoelastic jets can possess significant initial longitudinal viscoelastic stresses generated in the preceding flow domain (the transition zone between the Taylor cone and the thin jet zone) [18]. Such stresses can disrupt the agglomerates of zirconia nanoparticles and make a uniform dispersion of very fine nanoparticles. While, dispersion of nanoparticles into a polymeric matrix has ever been one of the major challenges in the fabrication of well defined nanocomposites, it seems that electrospinning at low filler concentrations can solve this problem minimizing the need to surface functionalization of the nanoparticles. However, as seen in Fig. 3C, for NFM7, most of the nanoparticles are located at the skin layer. This difference in distribution mode of the nanoparticles compared to the previous composition (i.e. NFM5) is due to the higher outward diffusion of the residual solvent induced by a higher applied voltage. Such a behaviour can also be considered as the cause of formation of a highly rough and porous surface of the fibers present at NFM7 in contrast to those of NFM5 (Fig. 2B Vs. 2A).

The aforementioned findings about nanofiber diameter variation and diameter distribution mode, nanofiber surface roughness and embedding of the nanoparticles might influence the mechanical and wettability performance of the membranes and thus can be of significant importance.

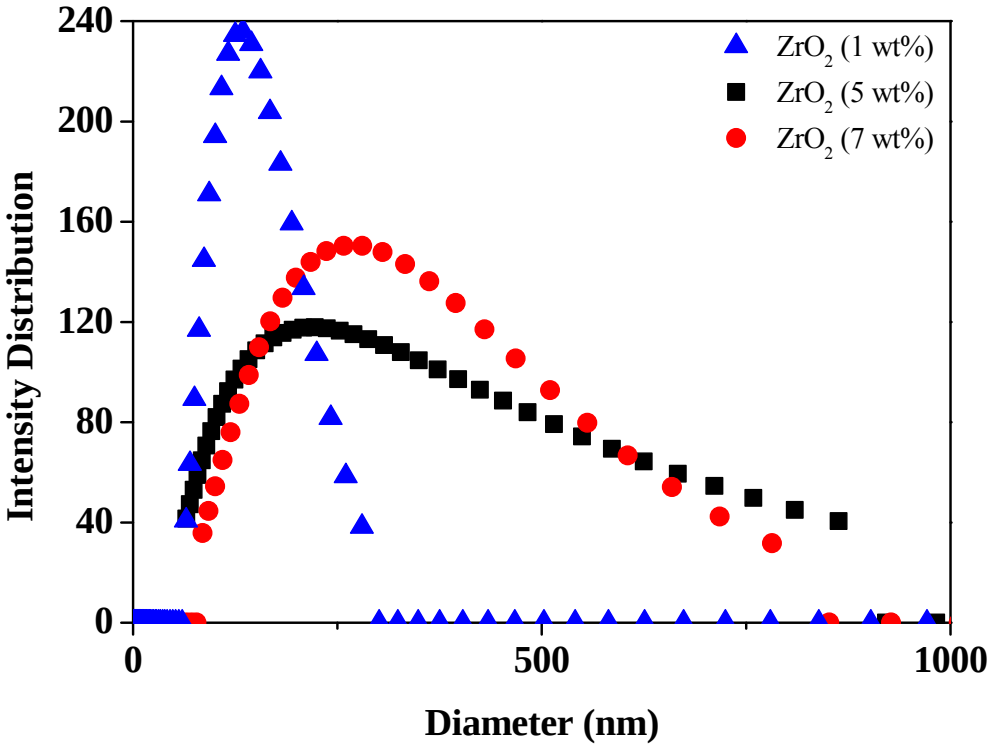
240
200
160
120
80
40
0
0
500
1000
Intensity Distribution
Diameter (nm)
ZrO2 (1 wt%)
ZrO2 (5 wt%)
ZrO2 (7 wt%)

(A)

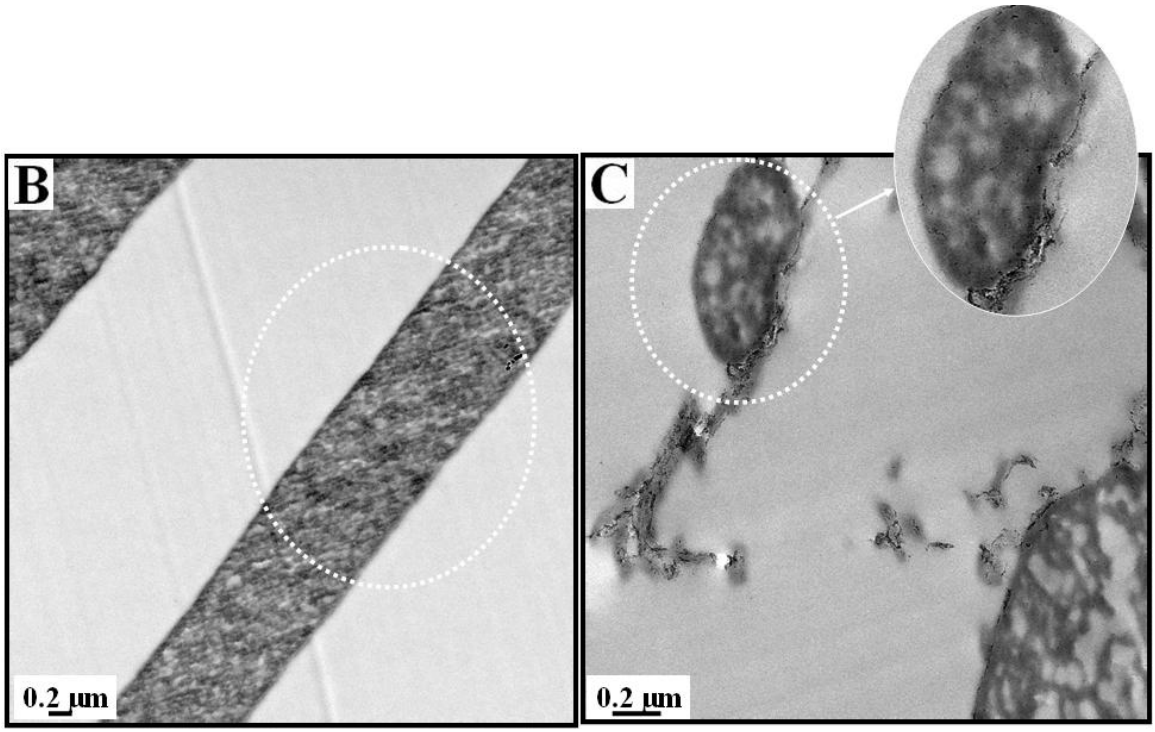
B
0.2 μm
C
0.2 μm

Fig. 3

3.2. Mechanical Properties

Keeping in mind the above mentioned influential factors alterations, we investigated the mechanical properties of the electrospun membranes through several mechanical tests including nanoindentation, tensile test and DMA.

3.2.1. Nanoindentation

Nanoindentation tests can give us an overview about the mechanical behaviour of the electrospun nanofibrous membranes especially about their compaction under a compressive force. The main desirable properties including recovery index (compaction), storage modulus (E') and the mean pressure ($\overline{P}$) are inferred from the obtained nanoindentation graphs shown in Fig. 4A.

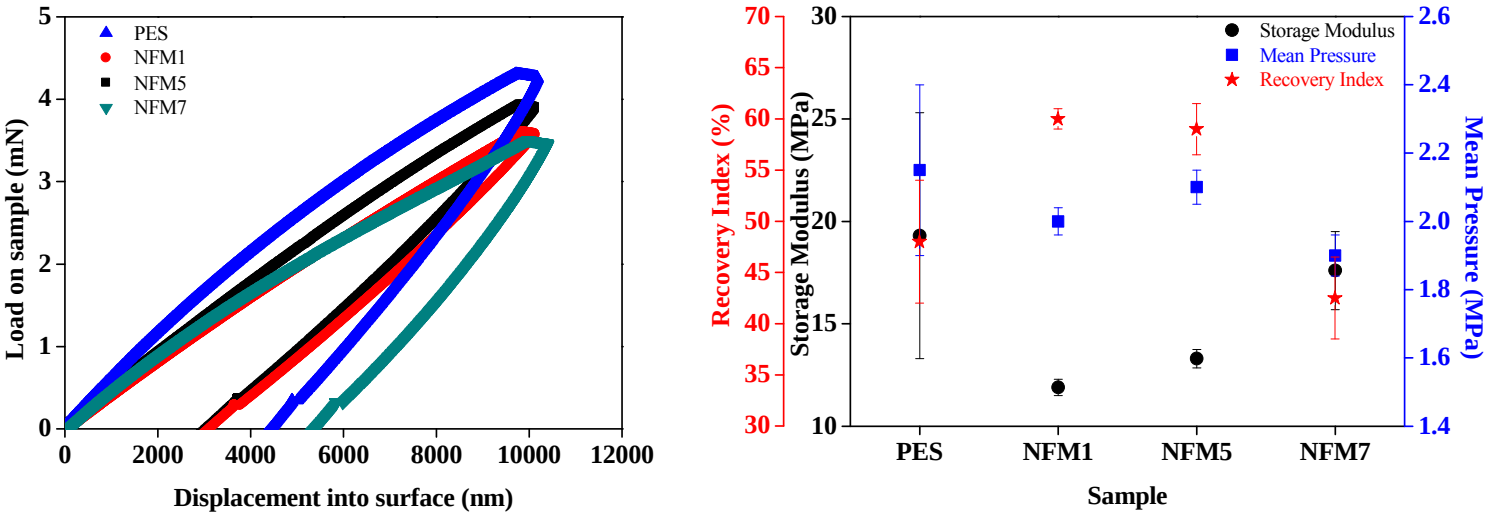

(A) (B)

Fig. 4

The recovery index of the PES electrospun nanofibrous membranes which shows the reciprocal magnitude of the compaction can be defined by Eq. (5):

$$I_r = \frac{(h_{\max} - h_f)}{h_{\max}} \times 100\,\% \qquad (5)$$

where, h_{max} and h_f represent the displacements at peak load and after complete unloading, respectively. The calculated recovery indices are presented in Fig. 4B. It is seen that addition of zirconia in NFM1 and NFM5 results in a higher recovery index i.e. a lower compaction. However, at NFM7, the composite nanofibers are compacted similar to the neat ones. The compaction behaviour primarily seems to be more influenced by two main parameters including nanofiller concentration and fiber diameter. A fibrous mat composing of the fibers with smaller diameter and higher nanofiller content is expected to undergo less compaction. Indeed, smaller fiber diameter means a severer stretching of the jet while electrospinning imposing a high molecular chain orientation along the fiber axis thereby a lower ductility [19]. But almost equal fiber diameters for the neat fibers and those of NFM1 and significant difference in their compaction values imply dependency of the compaction level to the nanofiller amount. However, the similar compaction values for the fibers of NFM1 and NFM5 and the lower value for those of NFM7 contradict to the previous conclusion. Apparently some more parameters are also influential on the compaction values. For instance, according to the TEM images (Fig. 3C) some agglomeration occur within the nanofibers of NFM7. Agglomeration decreases the interaction at the particle-polymer interface thereby inhibits an efficient load transfer. Additionally, agglomerates are weak points in the material and under stress they can break easily. A broken agglomerate then behaves as a strong stress concentrator [20-22].

Therefore a uniform dispersion of zirconia nanoparticles inside the nanofibers seems to be one of the main reasons for much lower compaction of NFM1 and NFM5. Besides agglomeration, surface roughnesses and pores (Fig. 2B) act as stress concentration points and make the fibers of NFM7 weaker than those of NFM5. Hence, the other main reason for the higher compaction resistance of NFM5 is the surface smoothness of the fibers. Such a high compaction resistance is very promising for filtration applications. A lower compaction means preservation of the porous structure of the membranes and as a result a more stable filtration efficiency during operation.

The storage modulus (E') of the electrospun nanofibrous mats can be inferred from the initial unloading contact stiffness (S), i.e. the slope of the initial part of the unloading curve by following Eq. (6) [23]:

$$E' = \frac{\sqrt{\pi}}{2\beta}\frac{S}{\sqrt{A}} \qquad (6)$$

where β is a constant that depends on the geometry of the indenter (β = 1 for a flat punch indenter). The calculated values of E' (Fig. 4B) imply higher storage moduli of the neat PES and NFM7 than those of NFM1 and NFM5. The most probable reason is the higher compaction and lower amount of porosity of these membranes [24, 25]. Naturally, among the two nanocomposite fibrous membranes with lower storage moduli i.e. NFM1 and NFM5, the latter shows a higher storage modulus mainly because of more amount of the dispersed nanofiller.

The mean pressure, $\overline{P}$, was determined from the maximum indentation load, P_{max}, divided by the contact area, A (Eq. (7)) [26]:

$$\overline{P} = \frac{P_{max}}{A} \qquad (7)$$

The mean pressure results (Fig. 4B) showed that the highest mean pressure belongs to the neat PES nanofibrous membrane mainly due to its high compaction and beaded nanofibers lowering porosity. Among the nanocomposite fibrous membranes, NFM5 and NFM7 show the highest and lowest mean pressures attributed to high effective amount of the nanofiller uniformly embedded into the nanofibers, smooth surface and uniform diameter distribution of the fibers of NFM5 versus high surface roughness and porosity of the fibers and agglomeration at NFM7.

3.2.2. Tensile Test and DMA

The electrospun nanofibrous membranes while dead-end and cross flow filtration modes are also exposed to tension stresses. The tensile performance of the nanocomposite PES fibrous membranes under static and dynamic forces were evaluated. According to the tensile test results (Fig. 5A), tensile strength, modulus and elongation of the PES nanofibrous membranes increase with addition of zirconia amount. The maximum magnitudes of such properties are seen at NFM5, while at NFM7 these properties decline compared to the previous composition indicating the important role of efficient nanoparticles embedding mode along with surface smoothness and the suppressing effect of surface roughness and porosity also agglomeration. A similar mechanical performance in terms of the storage and loss moduli is deduced from the DMA results (Figs. 5B&C). Moreover, for all the samples, the dynamic moduli show a constant linear trend independent to the applied frequencies.

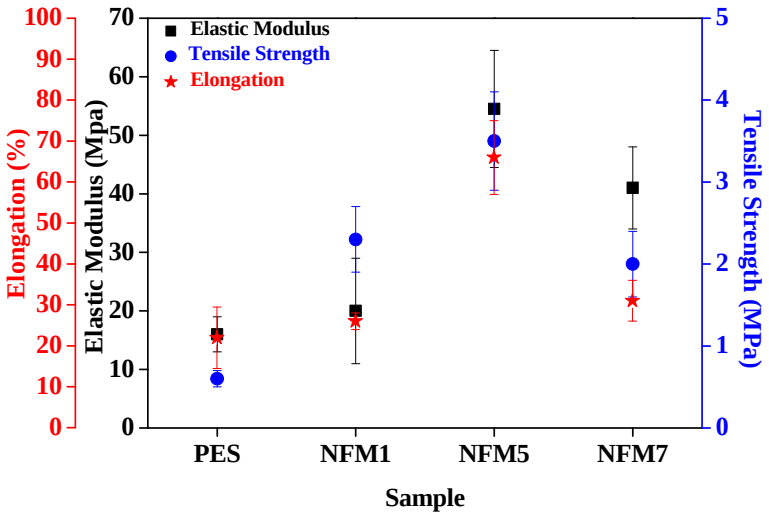

(A)

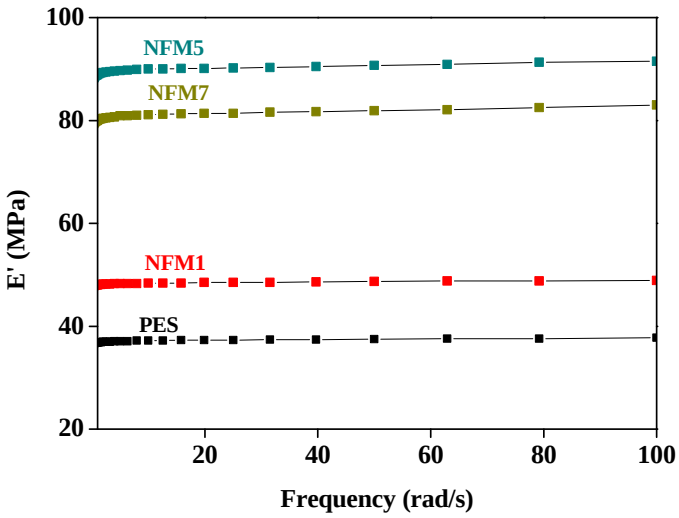

(B)

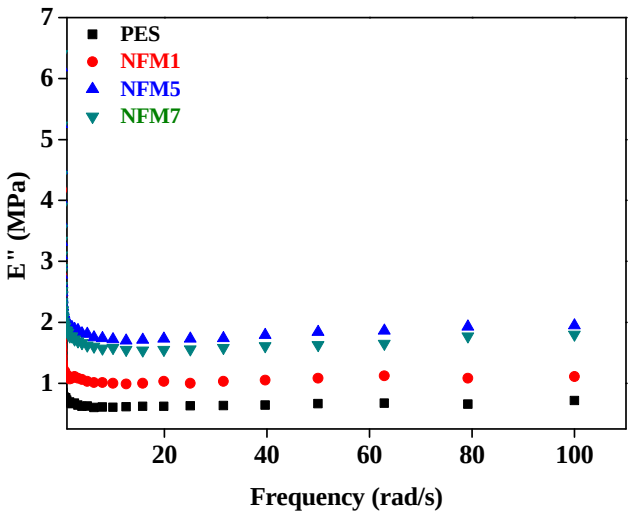

(C)

Fig. 5

Increase of loss modulus (damping) and elongation of the reinforced membranes is a very interesting and important finding implying high ductility i.e. low brittleness of the electrospun nanofibrous membranes after incorporation of the zirconia nanoparticles. This feature makes the ZrO_2/PES nanofibrous membranes superior to those filled with other ceramic nanoparticles e.g. SiO_2 [27].

3.3. Membrane wettability

For the hydrophobic PES electrospun nanofibrous membrane to be proposed for water filtration, in addition to the mechanical performance, wettability can also be a concern. Addition of zirconia nanoparticles could be also beneficial to increase wettability. Water contact angle (WCA) measurements (Fig. 6) imply a lower hydrophobicity of the ZrO_2/PES electrospun nanocomposite fibrous membranes as compared to the neat PES ones. The water contact angle of 120° for the neat PES nanofibrous membrane decreases to 105° for NFM5. The WCA of NFM7 is slightly higher than that of NFM5 due to the higher surface roughness of the fibers preventing a full contact with the water droplet.

In general, incorporation of polar ceramic nanoparticles such as zirconia is expected to make the hydrophobic membranes more hydrophilic. But this effect is only rather weak in our systems. Such performance can be attributed to embedding of the nanoparticles into the PES nanofibers. The zirconia nanoparticles are entrapped inside the nanofibers and can not be exposed on the surface mainly due to their much less and almost no solubility in the solvent and higher surface free energy than those of PES which induces formation of a solely polymeric coat layer on the jet and fibers [28]. Therefore, the nanoparticles are more beneficial in term of the mechanical properties rather than wettability.

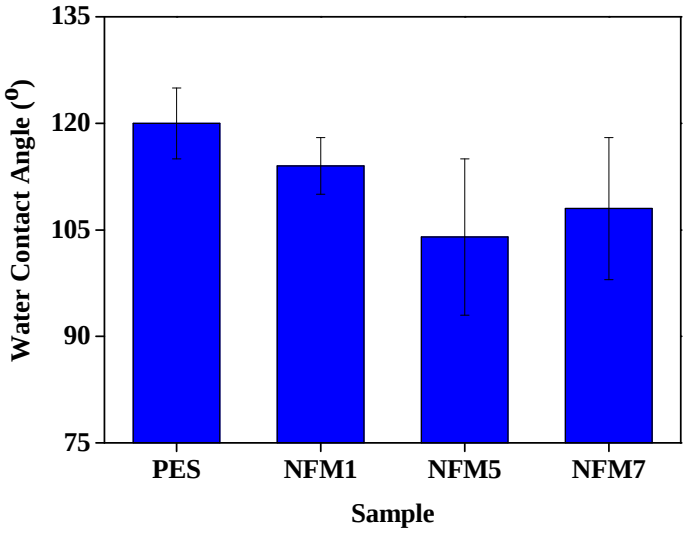

Fig. 6

3.4. Porosity and pore size

Formation of the larger beadless nanocomposite fibers as seen in Figs. 1 A-D could change the porous structure of the membranes. As shown in Fig. 7, addition of the ZrO_2 nanoparticles does not change the porosity significantly (less than 10%). Noteworthy, due to applying pressure for thickness measurement by the micrometer, the porosity values measured do not represent the real volume porosity which should be higher. Despite not so different porosity, the nanocomposite fibrous membranes show a bigger pore size than the neat ones especially at NFM5 and NFM7, attributed to the presence of larger beadless fibers. At a given areal density (~40 $x10^{-4}$ g/cm^2) and porosity, the fibers with bigger diameter create bigger pores [13]. Variation of porosity and pore size of the electrospun membranes could be influential on their permeability.

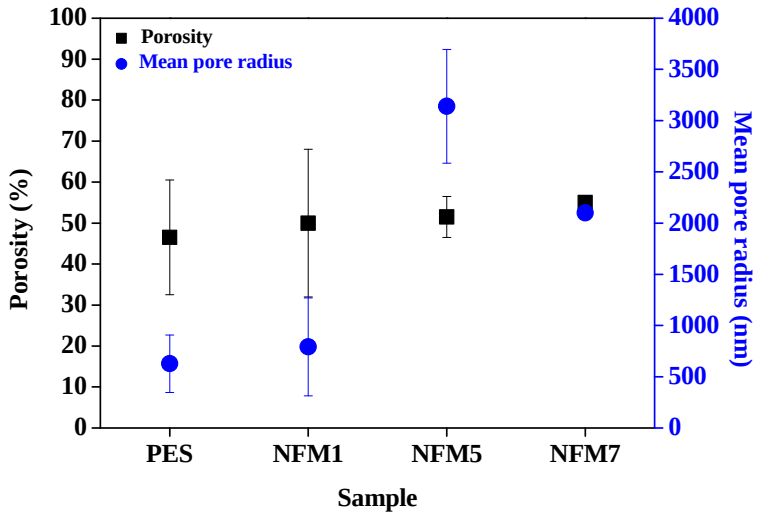

Fig. 7

3.5. Membrane permeability

Water flux measurements (Fig. 8) show a significantly ascending trend for the ZrO_2/ PES NFMs with a peak at NFM5. The results prove that addition of inorganic filler considerably enhances the permeability of the NFMs during filtration.

To discuss the permeance behaviour of the nanocomposite nanofibrous membranes, several influential factors including mechanical properties, wettability, porosity and pore size should be taken into account.

The permeance behaviour of the electrospun membranes can be described according to the Hagen-Poisseuille's equation (Eq. (8)) [29, 30]:

$$J = \frac{\varepsilon r^2}{8\mu\tau}\frac{\Delta P}{\Delta x} \qquad (8)$$

where J is the water flux (m^3/s), ε the porosity (-), r the pore radius (m), τ the tortuosity (-), ΔP the pressure difference across the membrane (Pa) (1 Pa=10^{-5} bar), μ the dynamic viscosity (Pa s) and Δx the membrane thickness (m).

According to this equation and considering almost constant porosity of all the membranes at different compositions (Fig. 7), increase of pore size (r) of the NFMs at higher zirconia concentrations can result in a higher flux. However, as seen in Fig.8, NFM1 despite an approximately equal pore size with the neat PES nanofibrous membrane, shows an almost two times higher water flux. This finding confirms that the main reason for such a rise in permeability is the enhanced mechanical properties e.g. compaction resistance obtained through embedding of the inorganic filler into the electrospun nanofibers. It is assumed that in case of compaction, nanofibrous layers approach to each other thereby interconnectivity of the pores declines i.e. tortuosity (τ) increases, in addition volume porosity and pore size (r) decreases leading to a higher membrane resistance and loss of permeability. Similarly, such a behaviour has been observed for conventional polymeric membranes while a pressure-driven liquid filtration as well [31]. However, when a membrane is compaction resistant, adverse effects mentioned above are inhibited and permeability is preserved.

Optimum mechanical performance e.g. compaction resistance along with an improved wettability also presence of bigger pores at the higher zirconia contents especially at NFM5 result in a significantly higher permeability.

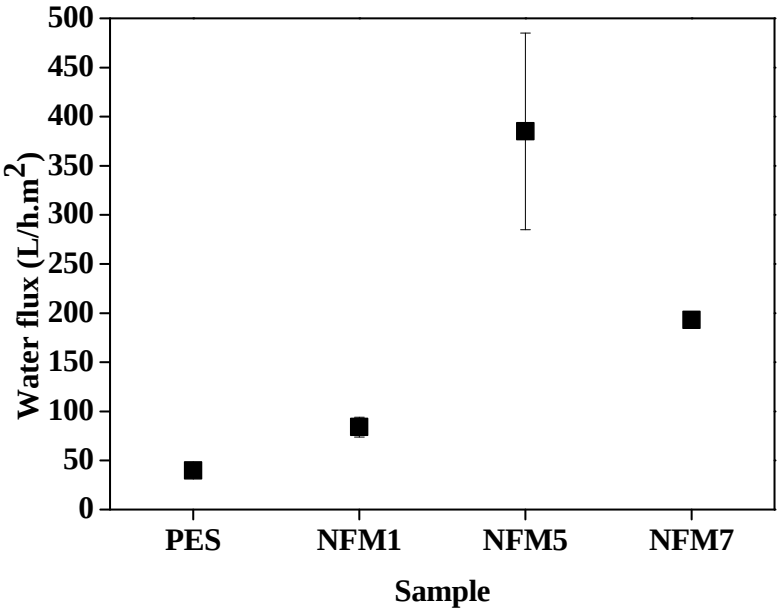

Fig. 8

3.6. Membrane selectivity

The structural modifications induced by addition of zirconia nanoparticles were included: no bead formation thereby slightly enhanced porosity, increase of fiber diameters hence pore size and optimized mechanical stability. All these changes could be influential on the retention ability of the nanocomposite fibrous membranes. Usually, the electrospun nanofibrous membranes owing to their pore size (100 nm-10 μm) are considered as microfiltration (MF) membranes in water treatment [32]. One important application of MF membranes is in removal of colloidal particles from water streams [33]. Therefore, to evaluate retention efficiency of the electrospun nanocomposite membranes developed in this study, they were utilized to separate colloidal particles from an aqueous nanosuspenion.

The results of the retention test in terms of retention efficiency also permeate flux are shown in Fig.9. All the membranes but NFM 5 showed a very optimum and

comparable retention efficiency proved by absence of any detectable particle inside the permeates i.e. an almost 100% efficiency (Fig. 9A). NFM5 indicated a less retention efficiency and nanoparticles were present in the permeate with smaller size than those within the feed. As shown in Fig. 9B, all the permeates other than that of NFM5 exhibit no turbidity comparable to the pure water sample. For NFM5, loss of turbidity compared to the feed, implies separation of a significant part (though not complete) of the suspended solids.

Permeate flux of the membranes follows a trend very similar to their water flux behaviour. This means that the NFMs including NFM1 and NFM7 can sustain their higher permeability compared to the neat membrane while showing a very optimum retention efficiency comparable to that of the PES electrospun membrane.

The average particle size of the TiO_2 nanoparticles in the feed is about 560 nm. The mean pore diameter of the membranes are: 1250 nm for the PES electrospun membrane, 1580 nm for NFM1, 6280 nm for NFM5 and 4200 nm for NFM7. Hence if we consider sieving (size exclusion effect) as the main separation mechanism of the electrospun membranes studied here, all the particles should pass through. But this is not the case and by no means the membranes are considered as screen filters. For the three groups of PES, NFM1 and NFM7 membranes, almost all the nanoparticles and for NFM5 some part of the nanoparticles are rejected by the membranes. When the particle size is in submicron range, the velocity of migration of the particles away from the surface of fibrous membranes is at its minimum. The particles are adsorbed to the nanofibers through direct interception, inertial impaction and diffusion (i.e. Brownian motion) [34]. In fact, the first group of nanoparticles are entrapped within the membranes by adsorption

to the nanofibers and the next particles join them constructing a dense cake layer initiated from depth of the membrane and grown upward to the surface. Thus, the membranes perform as a depth filter. As seen in Fig. 10 A-D, formation of the cake layer is responsible of loss of flux compared to the pure water flux values. However, the higher flux seen for NFM1 and NFM7 as compared to the neat PES membrane could be due to low compaction (i.e. lower tortuosity and higher volume porosity) and bigger pore size, respectively. NFM5 possesses the largest pores and due to bigger fiber diameters i.e. less surface area compared to the other fibrous membranes is unable to catch all the nanoparticles and make an integrated cake layer (Fig. 10C). This is interpreted as a lower retention efficiency and higher permeate flux than the other nanocomposite fibrous membranes.

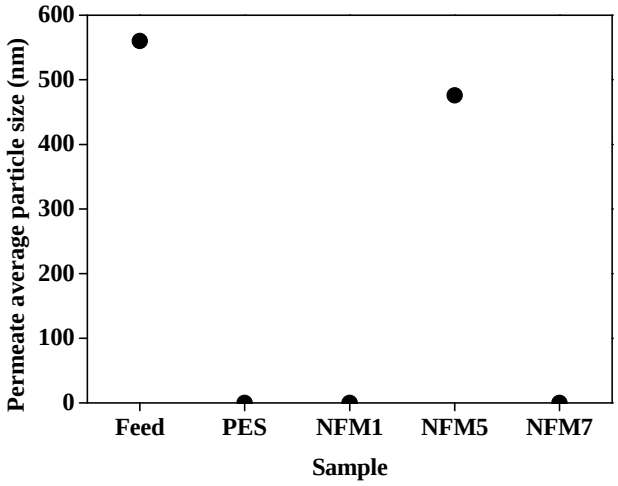

(A)

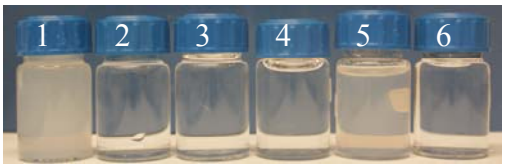

(B)

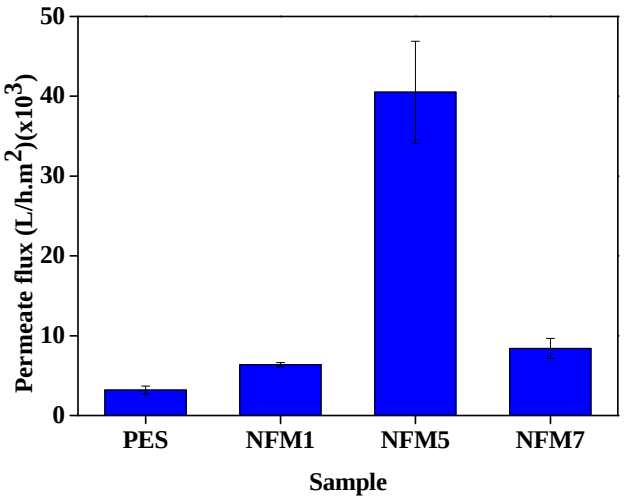
Permeate flux (L/h.m2)(x103)
50
40
30
20
10
0
PES
NFM1
NFM5
NFM7
Sample

(C)

Fig. 9

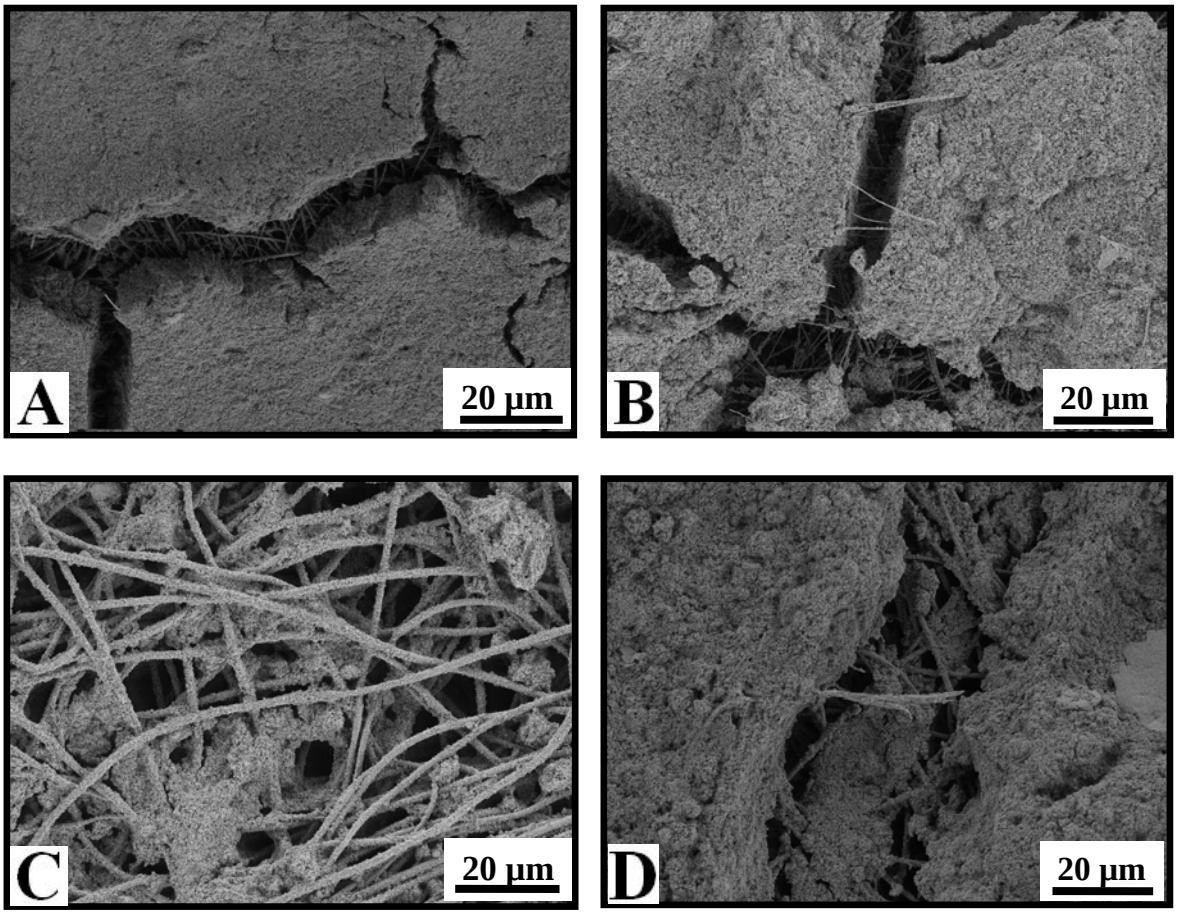
A
20 µm
B
20 µm
C
20 µm
D
20 µm

Fig. 10

4. Conclusions

We proved that mechanical stability of electrospun nanofibrous membranes during different modes of filtration such as dead-end and cross flow plays the major role in preservation of their very high permeance. In fact, to prevent any kind of compaction and disintegration resulting in failure and loss of efficiency, nanofibrous membranes should be somehow mechanically strengthened.

To do so, for the first time we reinforced PES electrospun nanofibrous membranes with zirconia nanoparticles. The nanocomposite fibrous membranes show an optimized filtration efficiency in terms of permeability and selectivity. Optimized permeability could be correlated to the enhanced mechanical properties of the membranes. This enhancement is caused by a good dispersion of the zirconia nanoparticles in the composite fibers rather than on the surface. These nanoparticles are not only excellent inherent mechanical modifiers, but also improve structural properties of the electrospun mats such as a smooth fiber surface, no bead defects and uniform diameter distribution. Improved wettability of this composite electrospun membranes, yet not so significant due to embedding of the nanoparticles, could contribute to a better water permeability as well.

This finding can assure us about the more efficient filtration performance of the nanocomposite PES nanofibrous membranes as compared to the neat PES ones. Mechanical reinforcement of such kind of highly porous membranes leads to preservation of their extraordinary water permeance, longer life span and lower energy consumption.

Acknowledgements

The authors would like to appreciate the financial support from a Helmholtz-DAAD PhD fellowship for S.Sh. Homaeigohar. Also, M. Elbahri thanks the initiative and networking fund of the Helmholtz Associations for providing the financial base of the start-up of his research group. Additionally, the authors would like to gratefully acknowledge Professor Volker Abetz for his useful comments on the manuscript, Dr. Erica T. Lilleodden (Institute of Materials Research of HZG) for her useful advices about nanoindentation, Kristian Bühr for design of the water flux measurement set-up, Heinrich Böttcher for tensile tests and DMA, Clarissa Abetz and Karen-Marita Prause for TEM and SEM measurements.

References

[1] Z.M. Huang, Y.Z. Zhang, M. Kotaki, S. Ramakrishna, Compos.Sci.Technol.63 (2003) 2223.
[2] C. Burger, B.S. Hsiao, B. Chu, Annu. Rev. Mater. Res. 36 (2006) 333.
[3] K. Yoon, B.S. Hsiao, B. Chu, Polymer 50 (2009) 2893.
[4] S.Sh. Homaeigohar, K. Buhr, K. Ebert, J. Mem. Sci. 365 (2010) 68.
[5] S.S. Choi, S.G. Lee, C.W. Joo, S.S. Im, S. Kim, J. Mater. Sci. 39 (2004) 1511.
[6] Z. Ma, M. Kotaki, S. Ramakrishna, J. Mem. Sci. 272 (2006) 179.
[7] M. Yanagioka, C. Frank, Macromolecules 41 (2008) 5441.
[8] S. Sh. Homaeigohar, H. Mahdavi, M. Elbahri, J. Colloid and Interface Sci. 366(2012) 51.
[9] J. Kim, B. V. d. Bruggen, Environ. Pollut. 158 (2010) 2335.
[10] L.Y. Ng, A.W. Mohammad, C.P. Leo, N. Hilal, Desalination In press (2011).
[11] J. Chevalier, Biomaterials 27 (2006) 535.
[12] H. Na, Y. Zhao, X. Liu, C. Zhao, X. Yuan, J. Appl. Polym. Sci.122 (2011) 774.
[13] S.J. Eichhorn, W. Sampson, J.R. Soc. Interface 2 (2005) 309.
[14] W. Sampson, J.Mater.Sci.38 (2003) 1617.
[15] H. Fong, I. Chun, D. Reneker, Polymer 40 (1999) 4585.
[16] O.S. Yördem, M. Papila, Y. Mencelog˘lu, Mater.Design 29 (2008) 34.
[17] K.M. Sawicka, P. Gouma, J. Nanopart. Res. 8 (2006) 769.
[18] T. Han, A.L. Yarin, D. Reneker, Polymer 49 (2008) 1651.
[19] Z. Chen, B. Wei, X. Mo, C.T. Lim, S Ramakrishna, F. Cui, Mater. Sci Eng;C 29 (2009) 2428.
[20] R. Roger (Ed.) Particulate-filled Polymer Composites, Rapra Technology Limited, Shrewsbury, 2003.
[21] E.N. Lawrence, F. Robert (Eds.), Mechanical Properties of Polymers and Composites, Marcel Dekker, New York, 1994.

[22] S.Sh. Homaeigohar, A. Yari Sadi, J. Javadpour, A. Khavandi, J. Euro. Cer. Soc. 26 (2006) 273.
[23] G.M. Odegard, T.S. Gates, H. Herring, Exper. Mech. 45 (2005) 130.
[24] R. Pal, J. Compo. Mater. 39 (2005) 1147.
[25] G. Lu, G.Q. Lu, Z. Xiao, J. Por. Mater. 6 (1999) 359.
[26] X. Li, B. Bhushan, Mater. Character. 48 (2002) 11.
[27] Y.-J. Kim, C. H. Ahn, M. B. Lee, M.-S. Choi, Mater.Chem.Phys.127 (2010) 137.
[28] B. O. Leung, A. P. Hitchcock, J. L. Brash, A. Scholl, A. Doran, Macromolecules 42 (2009) 1679.
[29] B. Van der Bruggen, C. Vandecasteele, T. Van Gestel, W. Doyen, R. Leysen, Environ. Progress 22 (2003) 46.
[30] K. Yoon, K. Kim, X. Wang, D. Fang, B.S. Hsiao, B. Chu, Polymer 47 (2006) 2434.
[31] K. M. Persson, V. Gekas, G. Tragardh, J.Mem.Sci. 100 (1995) 155.
[32] R. Baker, Membrane technology and applications, Wiley, 2004.
[33] S. Ramakrishna, R. Jose, P. S. Archana, A. S. Nair, R. Balamurugan, J. Venugopal, W. E. Teo, J. Mater. Sci. 45 (2010) 6283.
[34] R. Gopal, S. Kaur, C. Y. Feng, C. Chan, S. Ramakrishna, S. Tabe, T. Matsuura, J. Mem. Sci. 289 (2007) 210.

Figure captions:

Fig. 1 Surface morphology, bead formation and size (diameter) distribution of the PES nanofibers in the nanofibrous mats with and without presence of the zirconia particles (inset pictures have a 2 μm scale bar): A) the PES nanofibrous mat B) NFM1 C) NFM5 D) NFM7 E) the diameter distribution of the neat and nanocomposite PES fibrous mats

Fig. 2 SEM micrographs showing surface morphology of the nanocomposite fibers; Smooth surface versus rough and porous surface of the fibers of A) NFM5 B) NFM7, respectively;

Fig. 3 A)Particle size distribution of zirconia particles in the suspensions prepared for electrospinning ; TEM pictures showing embedding of very fine nanoparticles inside the fibers of B) NFM5 C) NFM7

Fig. 4 A) the load-displacement curve obtained by nanoindentation test for the ZrO_2 /PES nanofibrous mats

B) the storage modulus, mean pressure and recovery index of ZrO_2 /PES nanofibrous mats obtained by nanoindentation test

Fig. 5 Tensile properties of the neat and reinforced PES electrospun nanofibrous mats A) tensile test results ;B) dynamic storage modulus ;C) dynamic loss modulus

Fig. 6 Water contact angle measured for the neat and reinforced PES electrospun nanofibrous mats

Fig. 7 Porosity and pore size measurement for the neat and reinforced PES electrospun nanofibrous mats

Fig. 8 The water flux measured for the neat and reinforced PES electrospun nanofibrous mats

Fig. 9 Retention ability of the neat and reinforced PES electrospun nanofibrous mats A) retention efficiency ; B) visual comparison of turbidity level of the feed and permeate samples (1: feed, 2: pure water, 3: the permeate of the PES nanofibrous membrane, 4:the permeate of NFM1, 5:the permeate of NFM5 and 6: the permeate of NFM7) ;C)permeate flux

Fig. 10 The cake layer of the separated TiO_2 nanoparticles formed on the surface of the membranes including: A) Neat PES ; B) NFM1 ; C) NFM5 ; D) NFM7